PHYSICAL REVIEW A **67**, 012503 (2003)

Evaluation of the low-lying energy levels of two- and three-electron configurations for multicharged ions

O. Yu. Andreev,[1] L. N. Labzowsky,[1] G. Plunien,[2] and G. Soff[2]
[1]*Institute of Physics, St. Petersburg State University, Ulyanovskaya 1, 198904 Petrodvorets, St. Petersburg, Russia*
[2]*Institut für Theoretische Physik, Technische Universität Dresden, Mommsenstraße 13, D-01062 Dresden, Germany*

(Received 10 July 2002; published 22 January 2003)

Accurate QED evaluations of the one- and two-photon interelectron interaction for low-lying two- and three-electron configurations for ions with nuclear charge numbers $60 \leqslant Z \leqslant 93$ are performed. The three-photon interaction is also partly taken into account. The Coulomb gauge is employed. The results are compared with available experimental data and with different calculations. A detailed investigation of the behavior of the energy levels of the configurations $1s_{1/2}2s_{1/2}\,{}^1S_0$, $1s_{1/2}2p_{1/2}\,{}^3P_0$ near $Z=64$ and $Z=92$ is carried out. The knowledge of the exact energy difference near these regions is important for the future experimental search for parity nonconserving effects in highly charged ions.

DOI: 10.1103/PhysRevA.67.012503 PACS number(s): 31.30.Jv, 31.10.+z

I. INTRODUCTION

During the most recent years the energy levels of two- and three-electron configurations have been under very intensive experimental and theoretical investigation.

Accurate calculations of the energy levels for the two-electron configurations $1s_{1/2}2s_{1/2}\,{}^1S_0$, $1s_{1/2}2p_{1/2}\,{}^3P_0$, and $1s_{1/2}2s_{1/2}\,{}^3S_1$ have already been performed in Refs. [1,2]. In these papers the interelectron interaction has been considered in various approximations: on the basis of variational Schrödinger-wave functions with the inclusion of relativistic correlations [1] and using the relativistic many-body perturbation theory (RMBPT) [2]. For a long time these approaches defined the standard concerning the level of accuracy. In recent years, due to new developments in experimental and theoretical methods, the necessity to improve the accuracy of calculations has become urgent. Recently, rigorous QED evaluations of two-photon exchange corrections for low-lying configurations [3,4] have been performed.

First calculations of the energy levels for the three-electron configuration have been presented in Refs. [5–9]. As in the early papers on two-electron ions in these calculations the two- and many-photon exchanges have been considered approximately. Complete QED calculations of the two-photon exchange for three-electron ions have been performed in Refs. [10,4]. Within the framework of RMBPT the three-photon exchange has also been taken into account in Refs. [11,10,4].

In this paper we present an extension of previous calculations for two- and three-electron ions [4] for a variety of Z values. Here we include also the evaluations for the $1s_{1/2}2p_{1/2}\,{}^3P_0$ level, which have not been performed in Ref. [4]. Special attention has been paid to elaborate the behavior of the $1s_{1/2}2s_{1/2}\,{}^1S_0$ and $1s_{1/2}2p_{1/2}\,{}^3P_0$ levels near $Z=64$ and $Z=92$, where they become very close to each other. Accordingly, these system become suitable for monitoring parity-nonconserving (PNC) effects. Intensive experimental investigations of PNC effects in two-electron highly charged ions are under way [12–15]. The preparation of such experiments requires a precise knowledge of the exact difference between these energy levels.

II. THEORY

In this paper we evaluate corrections to the energy levels due to photon exchange. To calculate these corrections we employ the adiabatic S-matrix approach [16,17] and the line profile approach (LPA) [18]. Both methods are based on the Furry picture [19], which describes the many-electron atom as a set of bound electrons, moving in the external field of the nucleus and interacting with each other via the exchange of photons. With the aid of the Feynman rules for bound-state QED [20,21] the processes giving rise to corrections to the energy levels can be represented in terms of Feynman graphs. The photon-exchange corrections evaluated in this paper are depicted in Figs. 1–5.

As it has been shown in Refs. [22,20] the S-matrix approach is best suited for the evaluation of corrections described by the irreducible parts of the diagrams. However, its application to the evaluation of the reducible parts becomes rather complicated. Accordingly, for calculating the reducible parts we utilized the LPA. For a detailed description and for

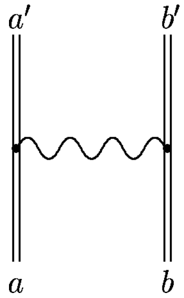

FIG. 1. Feynman graph describing the first-order interelectron interaction.The double solid lines correspond to bound electrons in the field of the nucleus, the wavy line corresponds to the sum of the Coulomb and Breit (transverse) photons. If $a'=a$ and $b'=b$ the graph is called "direct," in case $a'=b$, $b'=a$ we call it an "exchange" graph. The latter should be understood in connection with permutation symmetry.

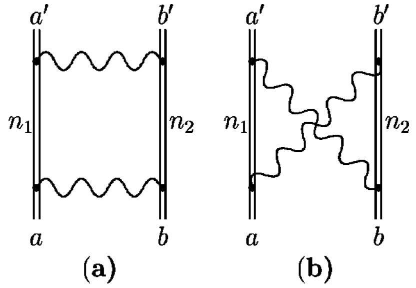

(a) (b)

FIG. 2. Feynman graphs describing the second-order interelectron interaction. The graph (a) is called "box" and the graph (b) is called "cross." Notations are the same as in Fig. 1. By n_1, n_2 the summation over intermediate states is indicated.

the application of this method we refer to Ref. [4].

The Coulomb gauge will be used throughout this paper. The photon propagators for Coulomb $(g=c)$ and transverse $(g=t)$ photons are given by Refs. [20,21]:

$$D^{g}_{\mu_1\mu_2}(x_1,x_2)=\frac{1}{2\pi i}\int_{-\infty}^{\infty}d\Omega\, I^{g}_{\mu_1\mu_2}(\Omega,r_{12})e^{i\Omega(t_1-t_2)} \tag{1}$$

together with the temporal Fourier transforms

$$I^{c}_{\mu_1\mu_2}(\Omega,r_{12})=\frac{\delta_{\mu_1 4}\delta_{\mu_2 4}}{r_{12}} \tag{2}$$

and

$$I^{t}_{\mu_1\mu_2}(\Omega,r_{12})=\left(\frac{\delta_{\mu_1\mu_2}}{r_{12}}e^{i|\Omega|r_{12}}+\nabla_{1\mu_1}\nabla_{2\mu_2}\frac{1}{r_{12}}\,\frac{1-e^{i|\Omega|r_{12}}}{|\Omega|^2}\right)(1-\delta_{\mu_1 4})(1-\delta_{\mu_2 4}). \tag{3}$$

A. The two-electron configurations

At first we consider the photon-exchange corrections for two-electron configurations. The wave function of a two-electron configurations is represented by

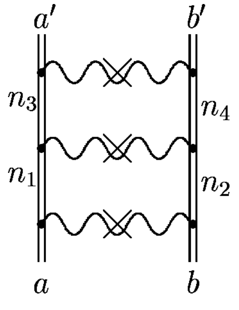

FIG. 3. The third-order "box" Feynman graph. The notations are the same as in Figs. 1 and 2. Here the wavy lines with the cross denote the sum of the Coulomb and unretarded Breit interaction.

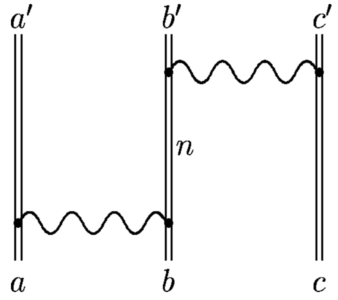

FIG. 4. The second-order "step" graph for three-electron ions. The notations are the same as in Figs. 1 and 2.

$$\Psi_{JMj_1j_2l_1l_2}(\mathbf{r}_1,\mathbf{r}_2)=N\sum_{m_1m_2}\mathrm{C}^{j_1j_2}_{JM}(m_1m_2)\times[\psi_{j_1l_1m_1}(\mathbf{r}_1)\psi_{j_2l_2m_2}(\mathbf{r}_2)-\psi_{j_1l_1m_1}(\mathbf{r}_2)\psi_{j_2l_2m_2}(\mathbf{r}_1)], \tag{4}$$

where $N=1/2$ for equivalent electrons and $N=1/\sqrt{2}$ for nonequivalent electrons, $\mathrm{C}^{j_1j_2}_{JM}(m_1m_2)$ is a Clebsch-Gordan symbol. By means of Eq. (4) we can specify the configuration $1s2s\,^3S_1$ by setting a, $b=1s_+,\ 2s_+$, where ± denote the two different projections of the total electron angular momentum, and we can derive the energy corrections according to the formula

$$\Delta E(1s2s\,^3S_1)=F_{1s_+2s_+;1s_+2s_+}, \tag{5}$$

$$F_{ab;cd}=F_{abcd}-F_{bacd}. \tag{6}$$

Here $F_{ab\ldots}$ denotes a function of one-electron states which are described by wave functions $\psi_a,\psi_b,\ldots$. The form of the function F depends on the type of Feynman graph under

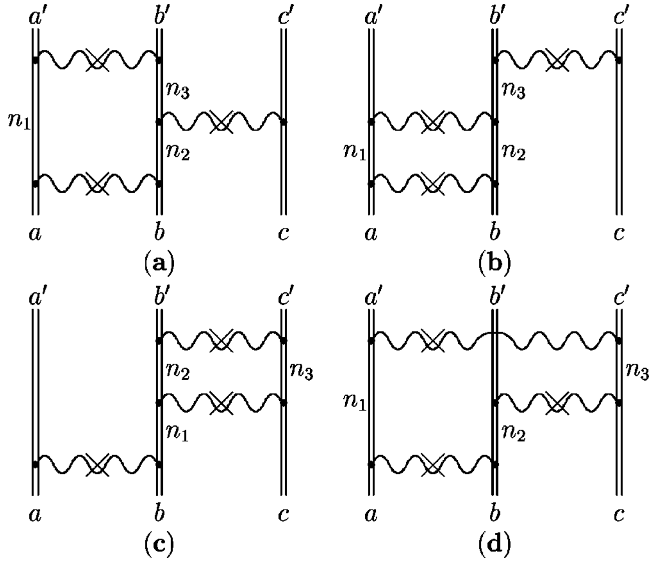

(a) (b) (c) (d)

FIG. 5. The third-order "step-box" graphs. The wavy line with the cross denotes the sum of the Coulomb and unretarded Breit interactions. Otherwise, the notations are the same as in Figs. 1–3.

consideration (see below). For the electron configurations $1s2s\,^1S_0$ and $1s2p\,^1P_0$ the energy corrections are given by

$$\Delta E(1s2s\,^1S_0)=F_{1s_-2s_+;1s_-2s_+}-F_{1s_+2s_-;1s_-2s_+} \tag{7}$$

and

$$\Delta E(1s2p\,^3P_0)=F_{1s_-2p_+;1s_-2p_+}-F_{1s_+2p_-;1s_-2p_+}, \tag{8}$$

respectively. The corrections due to one-photon exchange are represented by the graph in Fig. 1. This diagram is irreducible so that the *S*-matrix approach can be applied leading to

$$F^{(1)}_{a'b'ab}=\sum_g I^g(\varepsilon_{a'}-\varepsilon_a)_{a'b'ab}\,. \tag{9}$$

Here we have introduced the following notation [see definitions Eqs. (2) and (3)]:

$$I^g_{a'b'ab}(\Omega)\equiv\sum_{\mu_1\mu_2}\int\overline{\psi}_{a'}(\mathbf{r}_1)\overline{\psi}_{b'}(\mathbf{r}_2)\gamma^{(1)}_{\mu_1}\gamma^{(2)}_{\mu_2}I^g_{\mu_1\mu_2}(\Omega,r_{12})\times\psi_a(\mathbf{r}_1)\psi_b(\mathbf{r}_2)d^3r_1d^3r_2, \tag{10}$$

where the Dirac matrices $\gamma^{(i)}_{\mu_i}$ are acting on wave functions depending on spatial variables $\mathbf{r}_i$, respectively. For $g=c$ Eq. (9) determines the first-order Coulomb correction while for $g=t$ we obtain the first-order Breit correction.

The two-photon-exchange corrections are represented by the graphs in Fig. 2. The "box" diagram is reducible. Its reducible part is defined by the condition $\varepsilon_{n_1}+\varepsilon_{n_2}=\varepsilon_a+\varepsilon_b$. The "cross" diagram is irreducible. However, it is most convenient to extract the contribution with n_1, n_2 equal to a or b and to treat it like a reducible part of the "cross" diagram. Contributions due to states n_1, n_2 included in the reducible parts are called reference state contributions. Application of the *S*-matrix approach for calculating the irreducible part and of the LPA for the reducible part of the "box" and "cross" diagrams, respectively, results in the explicit formulas

$$F^{(2)(\text{box,irr})}_{a'b'ab}=\sum_{gg'}\sum_{n_1n_2}{}'\left\{\frac{i}{2\pi}\int_{-\infty}^{\infty}\frac{I^g(\Omega)_{a'b'n_1n_2}I^{g'}(\Omega-\varepsilon_{a'}+\varepsilon_a)_{n_1n_2ab}}{(\varepsilon_a+\varepsilon_b-\varepsilon_{n_1}-\varepsilon_{n_2})(\Omega-\varepsilon_{n_2}+\varepsilon_{b'}+i0\varepsilon_{n_2})}d\Omega\right.$$
$$\left.+\frac{i}{2\pi}\int_{-\infty}^{\infty}\frac{I^g(\Omega)_{b'a'n_1n_2}I^{g'}(\Omega-\varepsilon_a+\varepsilon_{a'})_{n_1n_2ba}}{(\varepsilon_a+\varepsilon_b-\varepsilon_{n_1}-\varepsilon_{n_2})(\Omega-\varepsilon_{n_2}+\varepsilon_{a'}+i0\varepsilon_{n_2})}d\Omega\right\}, \tag{11}$$

$$F^{(2)(\text{box,red})}_{a'b'ab}=-\frac{1}{2}\sum_{gg'}\sum_{n_1n_2}{}''\left\{\frac{i}{2\pi}\int_{-\infty}^{\infty}\frac{I^g(\Omega)_{a'b'n_1n_2}I^{g'}(\Omega-\varepsilon_{a'}+\varepsilon_a)_{n_1n_2ab}}{(\Omega-\varepsilon_{n_2}+\varepsilon_{b'}+i0\varepsilon_{n_2})^2}d\Omega\right.$$
$$\left.+\frac{i}{2\pi}\int_{-\infty}^{\infty}\frac{I^g(\Omega)_{b'a'n_1n_2}I^{g'}(\Omega-\varepsilon_a+\varepsilon_{a'})_{n_1n_2ba}}{(\Omega-\varepsilon_{n_2}+\varepsilon_{a'}+i0\varepsilon_{n_2})^2}d\Omega\right\}, \tag{12}$$

$$F^{(2)(\text{cross,irr})}_{a'b'ab}=\sum_{gg'}\sum_{n_1n_2}{}'\left\{\frac{i}{2\pi}\int_{-\infty}^{\infty}\frac{I^g(\Omega)_{b'n_2n_1a}I^{g'}(\Omega-\varepsilon_{a'}+\varepsilon_a)_{n_1a'bn_2}}{(\varepsilon_{n_2}-\varepsilon_{n_1}-\varepsilon_a+\varepsilon_{b'})(\Omega-\varepsilon_{n_2}+\varepsilon_a+i0\varepsilon_{n_2})}d\Omega\right.$$
$$\left.+\frac{i}{2\pi}\int_{-\infty}^{\infty}\frac{I^g(\Omega)_{n_1b'an_2}I^{g'}(\Omega-\varepsilon_{a'}+\varepsilon_a)_{a'n_2n_1b}}{(\varepsilon_{n_2}-\varepsilon_{n_1}+\varepsilon_a-\varepsilon_{b'})(\Omega-\varepsilon_{n_2}+\varepsilon_{b'}+i0\varepsilon_{n_2})}d\Omega\right\}, \tag{13}$$

$$F^{(2)(\text{cross,red})}_{a'b'ab}=\sum_{gg'}\sum_{n_1n_2}{}''\frac{i}{2\pi}\int_{-\infty}^{\infty}\frac{I^g(\Omega)_{b'n_2n_1a}I^{g'}(\Omega-\varepsilon_{a'}+\varepsilon_a)_{n_1a'bn_2}}{(\Omega-\varepsilon_{n_2}+\varepsilon_a+i0\varepsilon_{n_2})^2}d\Omega. \tag{14}$$

The prime at the summation symbols indicates that the reference states are excluded. The double prime indicates that only the reference state members are retained. In order to avoid division by zero in Eq. (13) in the case $a=b'$ and $n_1=n_2$, one has to take the limit $\varepsilon_{n_1}\to\varepsilon_{n_2}$ in both terms on the right-hand side. Thus the singularities cancel. It should be stressed that Eq. (14) coincides with the result of this limiting process. From Eqs. (12) and (14) it follows automatically that the corrections vanish for $g=g'=c$. The case $g=g'=c$ corresponds to the Coulomb-Coulomb correction, the case $g=g'=t$ determines the Breit-Breit and the case $g=c$, $g'=t$ or $g=t$, $g'=c$ refers to the Coulomb-Breit interaction.

For high-Z ions considered in this work the third-order contribution turns out to be small and it is sufficient to take into account its dominant part only. Accordingly, we consider only the third-order Coulomb and unretarded Breit "box" corrections. The corresponding Feynman graph is displayed in Fig. 3. The formula for the irreducible part of the third-order "box" correction can be derived in the same manner as for the corrections given by Eqs. (9) and (11). It takes the form

$$F^{(3)(\mathrm{box,irr})}_{a'b'ab}=\sum_{gg'g''}\sum_{n_1n_2n_3n_4}{}' \times\frac{I^{g}_{a'b'n_3n_4}I^{g'}_{n_3n_4n_1n_2}I^{g''}_{n_1n_2ab}}{(\varepsilon_{n_3}+\varepsilon_{n_4}-\varepsilon_{a'}-\varepsilon_{b'})(\varepsilon_{n_1}+\varepsilon_{n_2}-\varepsilon_a-\varepsilon_b)}, \tag{15}$$

where the prime indicates that the reference state contributions are excluded from the summation. Here the reference states are defined by the conditions $\varepsilon_{n_1}+\varepsilon_{n_2}=\varepsilon_a+\varepsilon_b$ or $\varepsilon_{n_3}+\varepsilon_{n_4}=\varepsilon_a+\varepsilon_b$. Applying the LPA to the graph in Fig. 3, we derive the following expression for the reducible part:

$$F^{(3)(\mathrm{box,red})}_{a'b'ab}=\sum_{gg'g''}\sum_{n_1n_2n_3n_4}{}'' I^{g}_{a'b'n_3n_4}I^{g'}_{n_3n_4n_1n_2}I^{g''}_{n_1n_2ab} \times\left\{\frac{(-1)}{2(\varepsilon_{n_3}+\varepsilon_{n_4}-\varepsilon_{a'}-\varepsilon_{b'})^2}+\frac{(-1)}{2(\varepsilon_{n_1}+\varepsilon_{n_2}-\varepsilon_a-\varepsilon_b)^2}\right\}, \tag{16}$$

where the double prime indicates that the summation is running only over the reference states. The terms leading to vanishing denominators in Eq. (16) should be omitted.

B. The three-electron configurations

Now we turn to three-electron ions. Here we consider three-electron configurations with a closed $(1s)^2$ shell, which can be described by the wave function

$$\Psi(\mathbf{r}_1,\mathbf{r}_2,\mathbf{r}_3)=\frac{1}{\sqrt{3!}}\sum_{i,j,k=1,2,3}\epsilon_{ijk}\psi_i(\mathbf{r}_1)\psi_j(\mathbf{r}_2)\psi_k(\mathbf{r}_3). \tag{17}$$

ϵ_{ijk} denotes the Levi-Civita symbol and $\psi_1(\mathbf{r})$, $\psi_2(\mathbf{r})$, and $\psi_3(\mathbf{r})$ denote one-electron wave functions.

As in the two-electron case we have to consider corrections represented by the two-electron Feynman graphs depicted in Figs. 1–3. Their contribution to the energy shift is given by

$$\Delta E(\{abc\})=F_{ab;ab}+F_{bc;bc}+F_{ca;ca}, \tag{18}$$

where $F_{ab;cd}$ is given by Eqs. (10) and (9)–(16). The set $\{abc\}$ is equal to the set $\{1s_+,1s_-,2s_{1/2+}\}$ for the configuration $(1s)^2 2s_{1/2}$ and to the set $\{1s_+,1s_-,2p_{1/2+}\}$ for the configuration $(1s)^2 2p_{1/2}$. The symbol ± refers to the different angular-momentum projections.

Besides the two-electron diagrams, in three-electron problem we have to take into account the additional three-electron Feynman graphs depicted in Figs. 4 and 5. The contribution of the three-electron graphs can be calculated according to

$$\Delta E(\{abc\})=\sum_{\substack{i',j',k'=1,2,3\\ i,j,k=1,2,3}}\epsilon_{i'j'k'}\epsilon_{ijk}F_{i'j'k'ijk}, \tag{19}$$

where the indices 1, 2, 3 at the F symbol must be replaced by *a*, *b*, *c* respectively, i.e., $F_{abcabc}\equiv F_{123123}$, etc. Equation (19) includes the contribution of the "direct" and all possible "exchange" diagrams which occur in the three-electron case.

Expressions for $F_{a'b'c'abc}$ corresponding to the graph in Fig. 4 are

$$F^{(2)(\mathrm{step,irr})}_{a'b'c'abc}=\sum_{gg'}\sum_{n}{}'\frac{I^{g}(\varepsilon_a-\varepsilon_{a'})_{na'ba}I^{g'}(\varepsilon_{c'}-\varepsilon_c)_{b'c'nc}}{\varepsilon_a+\varepsilon_b-\varepsilon_{a'}-\varepsilon_n}, \tag{20}$$

$$F^{(2)(\mathrm{step,red})}_{a'b'c'abc}=\sum_{gg'}\sum_{n}{}''\frac{\partial}{\partial\omega}[I^{g}(\varepsilon_a-\varepsilon_{a'}+\omega)_{na'ba}\times I^{g'}(\varepsilon_{c'}-\varepsilon_c+\omega)_{b'c'nc}]|_{\omega=0}, \tag{21}$$

where the prime at the summation symbol indicates that the summation runs over all n except for the case when the set of one-electron states $\{a',n,c\}$ is equivalent to the set $\{a,b,c\}$. The latter refers to reference states. The double prime implies that the summation runs over the reference states only. As for the two-electron contributions we have here $g,g'=c,t$. No reducible contribution arises for $g=g'=c$.

As it has been mentioned above, for the three-photon corrections, we take into account only their dominant parts, i.e., the third-order Coulomb and unretarded Breit "box" contributions. The corresponding three-electron Feynman graphs are displayed in Fig. 5. The formulas for the irreducible and the reducible parts of the third-order "box" correction are derived in the same manner as in Eqs. (15) and (16). The irreducible part can be expressed as

TABLE I. The values of nuclear root-mean-square radii employed in this work.

	${}^{142}_{60}$Nd	${}^{152}_{62}$Sm	${}^{153}_{63}$Eu	${}^{158}_{64}$Gd	${}^{159}_{65}$Tb	${}^{164}_{66}$Dy	${}^{166}_{68}$Er	${}^{174}_{70}$Yb	${}^{202}_{80}$Hg	${}^{231}_{91}$Pa	${}^{238}_{92}$U	${}^{237}_{93}$Np
$\langle r^2\rangle^{1/2}$ (fm)	4.914	5.032	5.041	5.090	5.099	5.224	5.165	5.317	5.467	5.700	5.860	5.744

$$F^{(3)(\text{step-box,irr})}_{a'b'c'abc}=\sum_{gg'g''}\sum_{n_1n_2n_3}{}' \frac{I^{g}_{a'b'n_1n_3}I^{g'}_{n_3c'n_2c}I^{g''}_{n_1n_2ab}}{(\varepsilon_{n_1}+\varepsilon_{n_3}-\varepsilon_{a'}-\varepsilon_{b'})(\varepsilon_{n_1}+\varepsilon_{n_2}-\varepsilon_a-\varepsilon_b)} +2\sum_{gg'g''}\sum_{n_1n_2n_3}{}' \frac{I^{g}_{b'c'n_3c}I^{g'}_{a'n_3n_1n_2}I^{g''}_{n_1n_2ab}}{(\varepsilon_{n_1}+\varepsilon_{n_2}-\varepsilon_a-\varepsilon_b)(\varepsilon_{n_3}+\varepsilon_{a'}-\varepsilon_a-\varepsilon_b)} +\sum_{gg'g''}\sum_{n_1n_2n_3}{}' \frac{I^{g}_{a'c'n_1n_3}I^{g'}_{b'n_3n_2c}I^{g''}_{n_1n_2ab}}{(\varepsilon_{n_1}+\varepsilon_{n_2}-\varepsilon_a-\varepsilon_b)(\varepsilon_{n_1}+\varepsilon_{n_3}-\varepsilon_{a'}-\varepsilon_{c'})}, \tag{22}$$

where the prime at the summation symbols indicates that the first summation does not run over states for which either the set $\{n_1,n_2,c\}$ or the set $\{n_1,n_3,c'\}$ are equivalent to the set $\{a,b,c\}$; the second summation does not run over the states for which the sets $\{n_1,n_2,c\}$ or $\{a',n_3,c\}$ are equivalent to the set $\{a,b,c\}$; and the third summation does not run over the states for which the sets $\{n_1,n_2,c\}$ or $\{n_1,n_3,b'\}$ are equivalent to the set $\{a,b,c\}$ (the cases of reference states). The reducible part of the third-order "step-box" corrections (see Fig. 5) can be cast into the form

$$F^{(3)(\text{step-box,red})}_{a'b'c'a'b'c'}=\sum_{gg'g''}\sum_{n_1n_2n_3}{}'' I^{g}_{a'b'n_1n_3}I^{g'}_{n_3c'n_2c}I^{g''}_{n_1n_2ab}\left\{\frac{(-1)}{2(\varepsilon_{n_1}+\varepsilon_{n_3}-\varepsilon_{a'}-\varepsilon_{b'})^2}+\frac{(-1)}{2(\varepsilon_{n_1}+\varepsilon_{n_2}-\varepsilon_a-\varepsilon_b)^2}\right\} +2\sum_{n_1n_2n_3}{}'' I^{g}_{b'c'n_3c}I^{g'}_{a'n_3n_1n_2}I^{g''}_{n_1n_2ab}\left\{\frac{(-1)}{2(\varepsilon_{n_1}+\varepsilon_{n_2}-\varepsilon_a-\varepsilon_b)^2}+\frac{(-1)}{2(\varepsilon_{n_3}+\varepsilon_{a'}-\varepsilon_a-\varepsilon_b)^2}\right\} +\sum_{n_1n_2n_3}{}'' I^{g}_{a'c'n_1n_3}I^{g'}_{b'n_3n_2c}I^{g''}_{n_1n_2ab}\left\{\frac{(-1)}{2(\varepsilon_{n_1}+\varepsilon_{n_2}-\varepsilon_a-\varepsilon_b)^2}+\frac{(-1)}{2(\varepsilon_{n_1}+\varepsilon_{n_3}-\varepsilon_{a'}-\varepsilon_{c'})^2}\right\}, \tag{23}$$

TABLE II. Different contributions to the total energy of the two-electron configuration $1s_{1/2}2s_{1/2}\,{}^1S_0$ (eV). The numbers present corrections to the ionization energy of the $2s_{1/2}$ electron with the opposite sign.

Z	Zero order	Nuclear size (NS)	1ph	2ph	3ph	SE with NS [29,30]	VP with NS [24,31]	SE screening [25]	VP screening [32]	Recoil [33]	Total
60	−13063.004	0.928	438.812	−4.781 −4.7721 [a]	0.026	11.409	−1.621	−0.257	0.092	0.055	−12618.341
62	−14015.106	1.201	458.300	−4.913	0.026	12.896	−1.893	−0.289	0.108	0.057	−13549.633
63	−14506.589	1.342	468.260	−4.980	0.026	13.700	−2.042	−0.304	0.116	0.058	−14030.413
64	−15008.567	1.519	478.371	−5.049	0.027	14.544	−2.201	−0.320	0.124	0.059	−14521.493
65	−15521.201	1.696	488.637	−5.120	0.027	15.427	−2.374	−0.335	0.132	0.060	−15023.051
66	−16044.661	1.968	499.061	−5.194	0.028	16.358	−2.557	−0.351	0.139	0.061	−15535.148
68	−17124.764	2.386	520.422	−5.350	0.029	18.363	−2.962	−0.382	0.161	0.064	−16592.033
70	−18250.361	3.099	542.484	−5.515	0.029	20.589	−3.419	−0.413	0.182	0.067	−17693.258
80	−24622.160	9.34	665.381	−6.504	0.038	35.391	−6.914	−0.651	0.352	0.086	−23925.641
91	−33320.132	32.50	832.758	−8.032	0.049	62.226	−14.632	−1.087	0.729	0.122	−32415.499
92	−34215.481	37.76	850.116	−8.184 −8.2131 [a]	0.052	65.418	−15.658	−1.127	0.777	0.127	−33286.200
93	−35130.460	40.94	868.029	−8.371	0.052	68.739	−16.770	−1.167	0.825	0.132	−34178.051

[a] From Ref. [34].

TABLE III. Different contributions to the total energy of the two-electron configuration $1s_{1/2}2p_{1/2}\,{}^3P_0$ (eV). The numbers present corrections to the ionization energy of the $2s_{1/2}$ electron with the opposite sign.

Z	Zero order	Nuclear size (NS)	1ph	2ph	3ph	SE with NS [29,30]	VP with NS [24,31]	SE screening [25]	VP screening [32]	Recoil [33]	Total
60	−13063.004	0.038	447.329	−4.068 −4.0645 [a]	0.013	0.298	−0.098	−0.112	0.031	0.050	−12619.523
62	−14015.106	0.052	468.642	−4.256	0.013	0.406	−0.124	−0.133	0.037	0.051	−13550.418
63	−14506.589	0.061	479.586	−4.354	0.014	0.469	−0.139	−0.144	0.040	0.052	−14031.004
64	−15008.567	0.071	490.731	−4.456	0.015	0.539	−0.155	−0.155	0.043	0.052	−14521.882
65	−15521.201	0.083	502.083	−4.561	0.016	0.615	−0.173	−0.165	0.046	0.053	−15023.204
66	−16044.661	0.099	513.649	−4.670	0.017	0.700	−0.193	−0.176	0.049	0.054	−15535.132
68	−17124.764	0.129	537.458	−4.888	0.019	0.899	−0.239	−0.197	0.058	0.055	−16591.470
70	−18250.361	0.180	562.218	−5.117 −5.1140 [a]	0.020	1.137	−0.297	−0.218	0.067	0.057	−17692.314
80	−24622.160	0.75	702.993	−6.598 −6.5959 [a]	0.034	3.234	−0.834	−0.416	0.143	0.068	−23922.786
91	−33320.132	3.68	902.031	−8.991	0.056	8.772	−2.451	−0.857	0.338	0.084	−32417.470
92	−34215.481	4.41	923.176	−9.274 −9.2760 [a]	0.058	9.550	−2.704	−0.897	0.365	0.086	−33290.711
93	−35130.460	4.93	944.984	−9.560	0.061	10.376	−2.982	−0.937	0.391	0.088	−34183.109

[a] From Ref. [3].

TABLE IV. Different contributions to the total energy of the two-electron configuration $1s_{1/2}2s_{1/2}\,{}^3S_1$ (eV). The numbers present corrections to the ionization energy of the $2s_{1/2}$ electron with the opposite sign.

Z	Zero order	Nuclear size (NS)	1ph	2ph	3ph	SE with NS [29,30]	VP with NS [24,31]	SE screening [25]	VP screening [32]	Recoil [33]	Total
60	−13063.004	0.928	333.849	−1.542 −1.5455 [a] −1.5459 [b]	−0.001	11.409	−1.621	−0.196	0.048	0.055	−12710.075
62	−14015.106	1.201	347.123	−1.562	−0.001	12.896	−1.893	−0.218	0.056	0.057	−13657.447
63	−14506.589	1.342	353.854	−1.572	−0.001	13.700	−2.042	−0.229	0.059	0.058	−14141.420
64	−15008.567	1.519	360.649	−1.582	−0.001	14.544	−2.201	−0.240	0.063	0.059	−14635.757
65	−15521.201	1.696	367.512	−1.593	0.000	15.427	−2.374	−0.251	0.067	0.060	−15140.657
66	−16044.661	1.968	374.442	−1.605	0.000	16.358	−2.557	−0.263	0.070	0.061	−15656.187
68	−17124.764	2.386	388.524	−1.626	0.000	18.363	−2.962	−0.285	0.080	0.064	−16720.220
70	−18250.361	3.099	402.904	−1.648 −1.6548 [a]	0.000	20.589	−3.419	−0.307	0.089	0.067	−17828.987
80	−24622.160	9.34	480.128	−1.789 −1.7956 [a]	0.000	35.391	−6.914	−0.470	0.162	0.086	−24106.226
91	−33320.132	32.50	578.374	−1.995	0.001	62.226	−14.632	−0.754	0.310	0.122	−32663.980
92	−34215.481	37.76	588.169	−2.018 −2.0203 [a] −2.0220 [b]	0.001	65.418	−15.658	−0.780	0.329	0.127	−33542.133
93	−35130.460	40.94	598.188	−2.040	0.001	68.739	−16.770	−0.806	0.347	0.132	−34441.729

[a] From Ref. [3].
[b] From Ref. [34].

TABLE V. Different contributions to the total energy of the three-electron configuration $(1s)^2 2s_{1/2}$ (eV). The numbers present corrections to the ionization energy of the $2s_{1/2}$ electron with the opposite sign.

Z	Zero order	Nuclear size (NS)	1ph	2ph	3ph	SE with NS [29,30]	VP with NS [24,31]	SE screening [35]	VP screening [36]	Recoil [33]	Total
60	−13063.004	0.928	720.180	−8.954	0.018	11.409	−1.621	−0.820	0.119	0.055	−12341.690
				−8.953 [a]	0.026 [b]						
62	−14015.106	1.201	749.835	−9.124	0.021	12.896	−1.893	−0.911	0.138	0.057	−13262.886
63	−14506.589	1.342	764.911	−9.213	0.023	13.700	−2.042	−0.957	0.147	0.058	−13738.620
64	−15008.567	1.519	780.160	−9.303	0.025	14.544	−2.201	−1.002	0.156	0.059	−14224.610
65	−15521.201	1.696	795.587	−9.395	0.027	15.427	−2.374	−1.048	0.166	0.060	−14721.055
66	−16044.661	1.968	811.194	−9.490	0.028	16.358	−2.557	−1.093	0.175	0.061	−15228.017
68	−17124.764	2.386	842.996	−9.690	0.029	18.363	−2.962	−1.205	0.200	0.064	−16274.583
70	−18250.361	3.099	875.598	−9.898	0.031	20.589	−3.419	−1.316	0.225	0.067	−17365.385
				−9.899 [a]	0.039 [b]						
80	−24622.160	9.34	1052.883	−11.143	0.043	35.391	−6.914	−2.063	0.418	0.086	−23544.119
				−11.147 [a]	0.055 [b]						
91	−33320.132	32.50	1283.940	−13.028	0.064	62.226	−14.632	−3.354	0.830	0.122	−31971.464
92	−34215.481	37.76	1307.306	−13.228	0.066	65.418	−15.658	−3.502	0.882	0.127	−32836.348 [c]
				−13.226 [a]	0.078 [b]						
93	−35130.460	40.94	1331.297	−13.441	0.069	68.739	−16.770	−3.650	0.934	0.132	−33722.210

[a] From Ref. [10].

[b] From Ref. [11].

[c] Nuclear polarization correction (−0.0377) [37,38] is included.

TABLE VI. Different contributions to the total energy of the three-electron configuration $(1s)^2 2p_{1/2}$ (eV). The numbers present corrections to the ionization energy of the $2p_{1/2}$ electron with the opposite sign.

Z	Zero order	Nuclear size (NS)	1ph	2ph	3ph	SE with NS [29,30]	VP with NS [24,31]	SE screening [35]	VP screening [36]	Recoil [33]	Total
60	−13063.004	0.038	875.619	−15.092	0.061	0.298	−0.098	−0.262	0.044	0.023	−12202.373
				−15.158 [a]	0.050 [b]						
62	−14015.106	0.052	913.798	−15.506	0.067	0.406	−0.124	−0.303	0.053	0.024	−13116.639
63	−14506.589	0.061	933.291	−15.726	0.071	0.469	−0.139	−0.324	0.057	0.025	−13588.804
64	−15008.567	0.071	953.066	−15.951	0.074	0.539	−0.155	−0.345	0.061	0.025	−14071.182
65	−15521.201	0.083	973.133	−16.182	0.077	0.615	−0.173	−0.365	0.066	0.026	−14563.921
66	−16044.661	0.099	993.500	−16.422	0.080	0.700	−0.193	−0.386	0.070	0.027	−15067.186
68	−17124.764	0.129	1035.185	−16.919	0.085	0.899	−0.239	−0.442	0.083	0.028	−16105.955
70	−18250.361	0.180	1078.206	−17.450	0.090	1.137	−0.297	−0.498	0.095	0.029	−17188.869
				−17.546 [a]	0.086 [b]						
80	−24622.160	0.75	1317.181	−20.827	0.142	3.234	−0.834	−0.931	0.203	0.038	−23323.204
				−20.828 [a]	0.131 [b]						
91	−33320.132	3.68	1642.274	−26.027	0.225	8.772	−2.451	−1.860	0.483	0.054	−31694.982
92	−34215.481	4.41	1676.142	−26.597	0.233	9.550	−2.704	−1.977	0.522	0.056	−32555.850 [c]
				−26.597 [a]	0.209 [b]						
93	−35130.460	4.93	1710.926	−27.232	0.245	10.376	−2.982	−2.095	0.560	0.057	−33435.675

[a] From Ref. [10].

[b] From Ref. [11].

[c] Nuclear polarization correction (−0.0039) [37,38] is included.

TABLE VII. Different theoretical data for the energy levels of two-electron configurations. The numbers present the ionization energy of the $2s_{1/2}$ or $2p_{1/2}$ electron with the opposite sign.

Contribution	$Z=60$	62	63	64	65	66	68	70
$E(2\,^1S_0)$								
This work	-12618.341	-13549.633	-14030.413	-14521.493	-15023.051	-15535.148	-16592.033	-17693.258
Drake [1]	-12618.188	-13549.412	-14030.191	-14521.251	-15022.780	-15534.938	-16591.716	-17692.948
Plante *et al.* [2]	-12618.629	-13549.909		-14521.817		-15535.580	-16592.446	-17693.778
$E(2\,^3P_0)$								
This work	-12619.523	-13550.418	-14031.004	-14521.882	-15023.204	-15535.132	-16591.470	-17692.314
Drake [1]	-12619.024	-13549.822	-14030.359	-14521.184	-15022.452	-15534.324	-16590.550	-17691.276
Plante *et al.* [2]	-12619.639	-13550.526		-14521.987		-15535.239	-16591.592	-17692.458
$E(2\,^3S_1)$								
This work	-12720.075	-13657.447	-14141.420	-14635.757	-15140.657	-15656.187	-16720.220	-17828.987
Drake [1]	-12720.166	-13657.533	-14141.506	-14635.845	-15140.741	-15656.359	-16720.343	-17829.187
Plante *et al.* [2]	-12720.253	-13657.628		-14635.951		-15656.475	-16720.473	-17829.334
$E(2\,^1S_0)-E(2\,^3P_0)$								
This work	1.182	0.785	0.591	0.389	0.153	-0.016	-0.563	-0.944
Drake [1]	0.835	0.411	0.168	-0.067	-0.328	-0.614	-1.166	-1.672
Plante *et al.* [2]	1.010	0.617		0.170		-0.341	-0.855	-1.320
$E(2\,^1S_0)-E(2\,^3S_1)$								
This work	101.734	107.814	111.007	114.264	117.606	121.039	128.187	135.729
Drake [1]	101.978	108.121	111.315	114.594	117.961	121.421	128.626	136.240
Plante *et al.* [2]	101.624	107.719		114.134		120.895	128.027	135.556
$E(2\,^3P_0)-E(2\,^3S_1)$								
This work	100.552	107.029	110.416	113.875	117.453	121.055	128.750	136.673
Drake [1]	101.143	107.710	111.147	114.661	118.290	122.035	129.793	137.911
Plante *et al.* [2]	100.614	107.102		113.963		121.236	128.882	136.876

where the double prime at the summation symbols indicates that the summations run over the corresponding reference states only [see the explanations for Eq. (22)]. It becomes evident that the contributions due to the graphs in Figs. 5(b,c) are equal. Therefore, we account for them by taking twice the contribution of the graph in Fig. 5(b).

III. NUMERICAL RESULTS AND DISCUSSION

The major result of the present work consists in the calculation of the two- and three-photon-exchange corrections to the energy levels of two-electron configurations 2^1S_0, 2^3P_0, 2^3S_1 and three-electron configurations $(1s)^2 2s_{1/2}$, $(1s)^2 2p_{1/2}$. The two-photon-exchange correction represents the leading part of the perturbation theory in second order. Accordingly, the main uncertainty of the theoretical values calculated earlier has been due to this correction.

In order to represent the Coulomb potential of the nucleus we employ a Fermi model for the nuclear density distribution

$$\rho(r)=\frac{N}{1+\exp[(r-c)/a]}, \tag{24}$$

where N is a normalization constant, $a=0.5350$ fm, and c is deduced via the equation

$$4\pi\int_0^\infty \rho(r)r^4dr=\langle r^2\rangle, \tag{25}$$

where $\langle r^2\rangle^{1/2}$ is the root-mean-square nuclear radius. In Table I we also display the values for the nuclear root-mean-square radii employed in this work. They have been taken from Ref. [23]. For nuclei with charge numbers Z not presented in Ref. [23] we utilize the empirical formula [24]

$$\langle r^2\rangle^{1/2}=(0.836\,A^{1/3}+0.570)\ \ \mathrm{fm}, \tag{26}$$

where A is the atomic mass number.

The results of our calculation of the two-photon-exchange correction are presented in Tables II –IV for two-electron configurations and in Tables V and VI for three-electron configurations. Our calculation is performed rigorously within the framework of QED. For details concerning the numerical procedure we refer to Ref. [4]. The accuracy of the present calculations is on the level of about 0.0001 a.u.

We have also taken into account the dominant part of the three-photon-exchange correction. Details of the approximation made were given in Sec. II. The results of the calculation for the three-photon-exchange correction are presented in Tables II –IV for two-electron configurations and in Tables V and VI for three-electron configurations. The correction caused by the exchange of three Breit photons is not

TABLE VIII. Different theoretical data for the energy levels of two-electron configurations. The numbers in the Table present the ionization energy of the $2s_{1/2}$ or $2p_{1/2}$ electron with the opposite sign, respectively.

Contribution	$Z=80$	91	92	93
$E(2\,^1S_0)$				
This work	-23925.641	-32415.499	-33286.200	-34178.051
Drake [1]	-23924.725	-32413.255	-33284.719	-34175.303
Plante *et al.* [2]	-23926.313	-13549.909	-33288.445	
$E(2\,^3P_0)$				
This work	-23922.786	-32417.470	-33290.711	-34183.109
Drake [1]	-23920.774	-32413.464	-33286.535	-34178.540
Plante *et al.* [2]	-23922.959	-13550.526	-33291.084	
$E(2\,^3S_1)$				
This work	-24106.226	-32663.981	-33542.134	-34441.730
Drake [1]	-24106.335	-32664.052	-33543.167	-34441.681
Plante *et al.* [2]	-24106.610		-33543.870	
$E(2\,^1S_0)-E(2\,^3P_0)$				
This work	-2.855	1.971	4.511	5.058
Drake [1]	-3.951	0.209	1.816	3.237
Plante *et al.* [2]	-3.354		2.640	
$E(2\,^1S_0)-E(2\,^3S_1)$				
This work	180.585	248.482	255.934	263.679
Drake [1]	181.610	250.796	258.448	266.378
Plante *et al.* [2]	180.297		255.425	
$E(2\,^3P_0)-E(2\,^3S_1)$				
This work	183.440	246.511	251.423	258.621
Drake [1]	185.561	250.587	256.632	263.141
Plante *et al.* [2]	183.651		252.786	

included since it was found to be less than 0.001 eV. In view of the approximation used to evaluate the three-photon-exchange correction, these values are given within an inaccuracy of about 10% [4].

In Tables II–IV we compile also all available corrections to the energy levels of the two-electron configurations under consideration. In order to compare our numerical data for the two-electron configurations $2\,^3P_0$ and $2\,^3S_1$ with other results in the literature we also provide values for the two-photon-exchange correction as it has been derived in Ref. [3]. We find that the data presented in Ref. [3] deviate from our results by not more than 0.0003 a.u.

Values for the energy of the three-electron configurations are presented in Tables V and VI. Comparing our results for the two-photon-exchange correction with data presented in Ref. [10], we achieved a very good agreement for the $(1s)^2 2s_{1/2}$ configuration. However, for the $(1s)^2 2p_{1/2}$ level we find a discrepancy of about 0.0035 a.u. for $Z=60$, 70. The three-photon-exchange correction is compared with the results obtained in Ref. [11]. In Ref. [11] the exchange of two and three Breit photons has been neglected.

The numbers for the recoil correction included in the tables for the total level energies of two- and three-electron configurations are obtained by interpolation for those Z values not calculated in the referred paper. The data for the self-energy (SE) screening and vacuum polarization (VP) screening of three-electron configurations as well as for the VP screening of two-electron configurations have been obtained via a similar interpolation. Results for the SE screening corrections of two-electron configurations have been obtained according to an approximate procedure which is based on the results provided in Ref. [25]. In particular, we refer to Table II of Ref. [25], where the self-energy screening functions $f(Z\alpha)$ for K- and L-shell single-electron states have been presented. From these values one can deduce the corresponding self-energy shift of a single-electron state due to the screening effect of another single-electron state. For example, we may denote by $E^{1\mathrm{s\ by\ }2\mathrm{s}}$ the screening correction to the $1s$-electron self-energy shift due to the $2s$-electron state and by $E^{2\mathrm{s\ by\ }1\mathrm{s}}$ the screening correction to the $2s$-electron self-energy originating from the $1s$-electron state, respectively. Accordingly, we suppose that the sum of the SE screening corrections $E^{^1S_0\ \mathrm{scr}}$and $E^{^3S_1\ \mathrm{scr}}$for the $^1S_0$ and $^3S_1$ configuration is represented by $E^{1\mathrm{s\ by\ }2\mathrm{s}}+E^{2\mathrm{s\ by\ }1\mathrm{s}}=E^{^1S_0\ \mathrm{scr}}+E^{^3S_1\ \mathrm{scr}}$. Then we suppose that $E^{^1S_0\ \mathrm{exch}}/E^{^3S_1\ \mathrm{exch}}=E^{^1S_0\ \mathrm{scr}}/E^{^3S_1\ \mathrm{scr}}$, where $E^{^1S_0\ \mathrm{exch}}$ and $E^{^3S_1\ \mathrm{exch}}$ are the first-order interelectron interaction corrections for the corresponding configurations. For the $^3P_0$ configuration we define $E^{1\mathrm{s\ by\ }2\mathrm{p}_{1/2}}+E^{2\mathrm{p}_{1/2}\mathrm{\ by\ }1\mathrm{s}}=E^{^3P_0\ \mathrm{scr}}$.

We did not include in our tables the values for the second-order radiative corrections. The reason is that they are only partly known for excited states. One can find the present status of these corrections in Ref. [26]. The last missing part of these corrections for the ground state (two-loop self-energy) has been evaluated recently in Ref. [27] for H-like uranium. However these corrections for $2s_{1/2}$, $2p_{1/2}$ states are not yet calculated, i.e., the inaccuracy associated with two-loop graphs in the evaluation of $2p_{1/2}$-$2s_{1/2}$ splitting for Li-like uranium remains. Therefore, the comparison of the theoretical results with the accurate experiment [28] given previously in Ref. [4] remains unaffected.

In Tables VII and VIII we present the total values for the energy levels of the two-electron configurations derived in this paper and compare them with the results of Refs. [1,2], respectively. The differences between the energy levels are also listed in that table. We should note that in Refs. [1,2], different approaches have been employed, i.e., the relativistic all-order theory (AO) [2] and the unified theory (UT) [1]. Compared with the rigorous QED approach, these theories involve several approximations, i.e., neglect of (i) negative-energy states, (ii) crossed photon contributions, and (iii) exact retardation effects. However, they account partially for higher-order interelectron interaction corrections. Accordingly, for highly charged ions the data compiled in Tables II–IV for the total corrections provide the most accurate theoretical predictions for the energy levels at present.

From the results presented in Tables VII and VIII one can conclude that the configurations $2\,^1S_0$ and $2\,^3P_0$ cross within the interval $60<Z<70$. The experimental investigation of PNC effects in heliumlike ions requires a precise knowledge of the energy difference between these levels at $Z=63$ [15]. The UT [1] predicts a value for this difference of about 0.168 eV, while the calculation presented in this paper gives a larger value of 0.591 eV. However, our calculations predict that the crossing of these levels takes place near $Z=66$ with an energy difference of about -0.016 eV. Nevertheless, the He-like Eu ion ($Z=63$) seems most suitable for the search of PNC effects [15]. We also investigated the splitting $E(2^1S_0)$-$E(2^3P_0)$ for two isotopes $^{151}_{63}$Eu and $^{153}_{63}$Eu and obtained an energy difference of 0.001 eV, which does not change the conclusions made in Ref. [15]. The present calculation also indicates that the other crossing point can be expected to be close to $Z=89,90$.

ACKNOWLEDGMENTS

The authors are indebted to Professor W. Nagel from the computer center of the TU Dresden for providing access to the all necessary computer facilities. O.Y.A. is grateful to the TU Dresden for the hospitality during his visits and to the DFG for financial support. The work of O.Y.A. and L.N.L. was supported by RFBR Grant No. 02-02-16578 and by Minobrazovanie Grant No. E00-3.1-7. G.P. and G.S. acknowledge financial support from BMBF, DFG, and GSI.

[1] G.W. Drake, Can. J. Phys. **66**, 586 (1988).
[2] D.R. Plante, W.R. Johnson, and J. Sapirstein, Phys. Rev. A **49**, 3519 (1994).
[3] P.J. Mohr and J. Sapirstein, Phys. Rev. A **62**, 052501 (2000).
[4] O.Yu. Andreev, L.N. Labzowsky, G. Plunien, and G. Soff, Phys. Rev. A **64**, 042513 (2001).
[5] W.R. Johnson, S.A. Blundell, and J. Sapirstein, Phys. Rev. A **37**, 2764 (1988).
[6] Y.K. Kim, D.H. Baik, P. Indelicato, and J.P. Desclaux, Phys. Rev. A **44**, 148 (1991).
[7] S. Blundell, P.J. Mohr, W.R. Johnson, and J. Sapirstein, Phys. Rev. A **48**, 2615 (1993).
[8] M.H. Chen, K.T. Cheng, W.R. Johnson, and J. Sapirstein, Phys. Rev. A **52**, 266 (1995).
[9] H. Persson, I. Lindgren, L.N. Labzowsky, G. Plunien, T. Beier, and G. Soff, Phys. Rev. A **54**, 2805 (1996).
[10] V.A. Yerokhin, A.N. Artemyev, V.M. Shabaev, M.M. Sysak, O.M. Zherebtsov, and G. Soff, Phys. Rev. A **64**, 032109 (2001).
[11] O.M. Zherebtsov, V.M. Shabaev, and V.A. Yerokhin, Phys. Lett. A **277**, 227 (2000).
[12] A. Schäfer, G. Soff, P. Indelicato, B. Müller, and W. Greiner, Phys. Rev. A **40**, 7362 (1989).
[13] V.V. Karasiev, L.N. Labzowsky, and A.V. Nefiodov, Phys. Lett. A **172**, 62 (1992).
[14] R.W. Dunford, Phys. Rev. A **54**, 3820 (1996).
[15] L.N. Labzowsky, A.V. Nefiodov, G. Plunien, G. Soff, R. Marrus, and D. Liesen, Phys. Rev. A **63**, 054105 (2001).
[16] M. Gell-Mann and F. Low, Phys. Rev. **84**, 350 (1951).
[17] J. Sucher, Phys. Rev. **107**, 1448 (1957).
[18] L. Labzowsky, V. Karasiev, I. Lindgren, H. Persson, and S. Salomonson, Phys. Scr. **T46**, 150 (1993).
[19] W.H. Furry, Phys. Rev. **81**, 115 (1951).
[20] L. Labzowsky, G. Klimchitskaya, and Yu. Dmitriev, *Relativistic Effects in the Spectra of Atomic Systems* (Institute of Physics, Bristol, 1993).
[21] L.N. Labzowsky, J. Phys. B **26**, 1039 (1993).
[22] M. G. Veselov and L. N. Labzowsky, *Teorija Atoma. Strojenie Elektronnykh Obolochek* (in Russian) [*Theory of Atoms. The Structure of the Electron Shells*] (Nauka, Moscow, 1986).
[23] T. Beier, Phys. Rep. **62**, 052501 (2001).
[24] W.R. Johnson and G. Soff, At. Data Nucl. Data Tables **33**, 405 (1985).
[25] P. Indelicato and P.J. Mohr, Phys. Rev. A **63**, 052507 (2001).
[26] P.J. Mohr, G. Plunien, and G. Soff, Phys. Rep. **293**, 227 (1998).
[27] V.A. Yerokhin and V.M. Shabaev, Phys. Rev. A **64**, 062507 (2001).
[28] J. Schweppe, A. Belkacem, L. Blumenfeld, N. Claytor, B. Feinberg, H. Gould, V.E. Kostroun, L. Levy, S. Misava, J.R. Mowat, and M.H. Prior, Phys. Rev. Lett. **66**, 1434 (1991).
[29] P.J. Mohr, Phys. Rev. A **46**, 4421 (1992).
[30] P.J. Mohr and G. Soff, Phys. Rev. Lett. **70**, 158 (1993).
[31] G. Soff and P.J. Mohr, Phys. Rev. A **38**, 5066 (1988).
[32] A.N. Artemyev, T. Beier, G. Plunien, V.M. Shabaev, G. Soff, and V.A. Yerokhin, Phys. Rev. A **62**, 022116 (2000).
[33] A.N. Artemyev, V.M. Shabaev, and V.A. Yerokhin, Phys. Rev. A **52**, 1884 (1995).
[34] B. Åsén, S. Salomonson, and I. Lindgren, Phys. Rev. A **65**, 032516 (2002).

[35] V.A. Yerokhin, A.N. Artemyev, T. Beier, G. Plunien, V.M. Shabaev, and G. Soff, Phys. Rev. A **60**, 3522 (1999).

[36] A.N. Artemyev, T. Beier, G. Plunien, V.M. Shabaev, G. Soff, and V.A. Yerokhin, Phys. Rev. A **60**, 45 (1999).

[37] G. Plunien and G. Soff, Phys. Rev. A **51**, 1119 (1995); **53**, 4614 (1996).

[38] A.V. Nefiodov, L.N. Labzowsky, G. Plunien, and G. Soff, Phys. Lett. A **222**, 227 (1996).